American Mineralogist, Volume 94, pages 657–665, 2009

Closure temperatures of intracrystalline ordering in anatectic and metamorphic hercynite, $Fe^{2+}Al_2O_4$

Barbara Lavina,[1,*] Bernardo Cesare,[2] Antonio M. Álvarez-Valero,[3] Hinako Uchida,[4] Robert T. Downs,[4] Anna Koneva,[5] and Przemyslaw Dera[1]

[1]Consortium for Advanced Radiation Sources, The University of Chicago, Chicago, Illinois 60637, U.S.A.
[2]Department of Geosciences, University of Padova, via Giotto 1, 35137 Padova, Italy
[3]Andalusian Institute of Earth Sciences (IACT, CSIC-Uni. Granada), Fuentenueva s/n, Faculty of Sciences, 18002, Granada, Spain
[4]Department of Geosciences, University of Arizona, Tucson, Arizona 85721-0077, U.S.A.
[5]Institute of Geochemistry, P.O. Box 4019, Irkutsk 664033, Russian Federation

Abstract

The closure temperature, T_C, of the intracrystalline ordering of Mg-hercynite is estimated with a comparative crystal-chemical approach. The single crystals were selected from two distinct geological environments that represent extremely different cooling rates. The fast cooled setting refers to anatectic metapelitic enclaves that occur in the high-K calc-alkaline lavas of the Neogene Volcanic Province of SE Spain. The slow cooled setting refers to metabauxite from the Anga metamorphic complex, Lake Baikal. Parameters sensitive to T_C include the oxygen fractional coordinate (u) and the inversion parameter (i). Experimental equilibration data on the spinel and hercynite end-members and on their solid solution are fitted to equations where T_C is given as a function of the hercynite content (Hc) of the solid solution and of u or i. The unavoidable simplifications made in this empirical approach are discussed. A reasonable value for T_C, ~400 °C, was obtained for the slow cooled metamorphic hercynite from the oxygen fractional coordinates. In contrast, an unreasonably high value of T_C, ~600 °C, was obtained from the inversion parameters. In the case of the fast cooled anatectic samples, T_C calculated from the two structural parameters are comparable; the five crystals show a range in the calculated values for T_C over ~250 °C, from ~700 to ~950 °C, which is reasonable considering the known diversity of cooling rates exhibited by their volcanic host-rocks.

Keywords: Hercynite, spinel, closure temperature

Introduction

This study explores the significance of the cation distribution of contrasting fast and slow cooled anatectic and metamorphic Mg-hercynite by comparing the ordering state of the natural samples with inversion-temperature data obtained from published literature. The equilibrium intracrystalline cation distribution in spinels is a function of the intensive thermodynamic parameters including temperature, pressure, and composition. Natural samples exhibit a non-equilibrium cation distribution that depends on the thermodynamic parameters controlling the equilibrium ordering and on the pressure-temperature-time path the crystals experienced. The ordering process involves short-range cation diffusion along with the breaking of bonds and a large kinetic barrier. Although pressure affects the inversion parameter (cf. Da Rocha and Thibaudeau 2003 for the spinel end-member), the effect of this variable is ignored in our model because the cation exchange processes experienced by the samples in this study occurred at either ambient or relatively low pressure (the pressure determined for garnet-biotite schists of the Anga metamorphic complex is 4–5 kbar, Makrygina et al. 2008).

The equilibrium temperature corresponding to the observed order state of a sample is called its closure temperature, T_C (Ganguly 1982); T_C provides insight on: (1) a lower limit of the maximum temperature that the rock experienced, and (2) a comparative cooling rate. The analyzed samples belong to two different geological environments representing slow and fast cooling rates experienced by Earth materials. Their inversion parameters and oxygen fractional coordinates are compared with available experimental data to estimate T_C.

The spinel structure exhibits a slightly distorted cubic close-packed array of oxygen atoms with cations occupying 1/8 of the available tetrahedral sites (T) and half of the octahedral sites (M). The chemical composition is generally represented as $^{T}(X_{1-i}Y_i)\,^{M}(X_iY_{2-i})O_4$, where X and Y represent divalent and trivalent cations in case of 2-3 spinels (or tetravalent and divalent cations in case of 4-2 spinels), respectively, and $0 \le i \le 1$ where i is the inversion parameter. In compounds where cations show strong site preferences, spinels can exhibit two ordered configurations, the normal state, with $i = 0$, and the inverse state, $i = 1$. Conversely, when the difference in site energy is not too great, the cation distribution shows partial disorder with intermediate values of i. The oxygen fractional coordinate (u), which is a measure of the oxygen packing distortion and is related to the ratio of the two polyhedral volumes, is known to be sensitive

* E-mail: lavina@cars.uchicago.edu

to the changes in the cation distribution. In the spinel-chromite solid solution, u is nearly constant for crystals that experienced the same thermal history (Princivalle et al. 1989; Della Giusta et al. 1996; Redfern et al. 1999). In X-ray diffraction studies, where it is difficult to distinguish occupancies of elements with similar X-ray scattering power, such as Mg and Al, variations in u are monitored to determine the cation distribution (cf. Andreozzi and Princivalle 2002). Harrison et al. (1998) demonstrated a non-linear relation between u and i for synthetic hercynite: $u = 0.26488 - 0.00118i - 0.0289i^2$.

The dependence of cation distribution on the equilibration temperature has been estimated for several end-members of the spinel group with various techniques (cf. Peterson et al. 1991; O'Neill et al. 1992; O'Neill and Dollase 1994; Redfern et al. 1999; Larsson et al. 1994; Harrison et al. 1998; Méducin et al. 2004), but relatively few studies have been conducted on solid solutions (cf. Della Giusta et al. 1986; Waerenborgh et al. 1994a, 1994b; Harrison et al. 1999; Andreozzi and Lucchesi 2002; Uchida et al. 2005). When samples have greater chemical complexity, the determination of the cation distribution becomes particularly challenging compared to simple chemical systems, but it is of much broader interest in geosciences because most of the natural rock-forming spinels are solid solutions of several end-members, and most important for the crust and upper mantle including: spinel s.s. ($MgAl_2O_4$)–hercynite ($FeAl_2O_4$)–chromite ($FeCr_2O_4$)–magnetite ($Fe^{2+}Fe^{3+}_2O_4$). A widely used method to determine cation distribution is X-ray diffraction, often complemented by Mössbauer spectroscopy (cf. Carbonin et al. 1996; O'Neill et al. 1992; Larsson et al.1994). Hålenius et al. (2002) suggested that some of the controversial Fe partitioning results in the literature may be ascribed to the low resolution of $^{IV}Fe^{2+}$ and $^{VI}Fe^{2+}$ absorption bands in Mössbauer spectra.

Hercynite exhibits a configuration close to a normal spinel, as exemplified by $i = 0.163(5)$ at 850 °C, (Hill 1984), with a quasi-linear increase of i with temperature, as shown by Larsson et al. (1994) using X-ray diffraction and Mössbauer spectroscopy and by Harrison et al. (1998) using in situ neutron diffraction. Harrison et al. (1998) pointed out that inconsistencies in the literature data on the temperature dependence of the cation distribution result from one or a combination of the following causes: (1) the fast rate of cation ordering in spinels, leading to observed cation distribution different from that at high annealing temperature because of imperfect quenching (Larsson et al. 1994); (2) the presence of Fe^{3+} ions, which have a large effect on crystal-chemical behavior of spinel (Hill 1984; Bohlen et al. 1986; Larsson et al. 1994); and/or (3) uncertainties in the interpretation of Mössbauer data because of the aforementioned low resolution of $^{IV}Fe^{2+}$ and $^{VI}Fe^{2+}$ absorption bands (Larsson et al. 1994). It has been pointed out that the fast rate of ordering could possibly result from the presence of cation vacancies (Larsson et al. 1994; Harrison and Putnis 1997). O'Neill (1994) studied $Co^{2+}Al_2O_4$ spinel because Co^{2+} and Fe^{2+} have similar crystal-chemical behavior, e.g., site preference energies (O'Neill and Navrotsky 1984), and because Co^{2+} and Co^{3+} have a larger energy gap than Fe^{2+} and Fe^{3+}, therefore, allowing to circumvent the problem of mixed valence states in the Co system. O'Neill (1994) showed that the rate of cation ordering in $CoAl_2O_4$ is similar to that found in other aluminate spinels, and concluded that the fast rate observed in $FeAl_2O_4$ is due to Fe^{3+}/vacancy defects. In addition to the factors listed above, X-ray scattering curves chosen for structure refinement also need to be taken into consideration. O'Neill and Dollase (1994) and Harrison et al. (1997) demonstrated that small differences in i can be observed in XRD refinement results depending on the choice of X-ray scattering curves, i.e., neutral atom, fully ionized, or half ionized. The cation distribution of synthetic samples along the spinel-hercynite join with a small Fe^{3+} component have been determined by Andreozzi and Lucchesi (2002) by single-crystal X-ray diffraction and Hålenius et al. (2002) by Mössbauer and electronic spectroscopy. The authors observed a disproportionate increase of ^{VI}Fe content from spinel s.s. to hercynite, leading to increasing $^{VI}Fe/Fe_{tot}$ along the join from 0 to 15.

Samples

Five single crystals of hercynite were selected from five different samples of anatectic metapelitic enclaves from the high-K calc-alkaline lavas of the Neogene Volcanic Province of SE Spain (hereafter H&M), and two from a metalaterite of the Anga metamorphic complex, Lake Baikal (hereafter BK).

Of the 5 anatectic enclaves, four (HO19, HO27BC, HO51, AVHz20) are from the locality of El Hoyazo (Cesare 1997; Álvarez-Valero et al. 2005; Álvarez-Valero and Kriegsman 2007; Acosta-Vigil et al. 2007), and one (AVMa8.9) is from Mazarrón (Cesare et al. 2003; Álvarez-Valero et al. 2007; Álvarez-Valero and Kriegsman 2007). The samples from El Hoyazo are typical spinel-cordierite rocks according to the definition of Zeck (1970). They are well-foliated, fine-grained, and contain the assemblage sillimanite–cordierite–K-feldspar–hercynite–graphite–ilmenite–biotite–glass±garnet±plagioclase. Hercynite forms euhedral porphyroblasts up to 1 mm across, statically overgrowing the foliation marked by fibrolitic sillimanite and graphite (Figs. 1a and 1b). The petrology of the HO19 enclave has been discussed in detail by Álvarez-Valero et al. (2005), whose genetic interpretations are probably applicable to all four of our samples from El Hoyazo. The most notable difference among the four enclaves from El Hoyazo is represented by the amount of biotite: HO27BC and HO51 are almost devoid of biotite, whereas AVHz20 and HO19 are biotite-rich. Biotite, intergrown with feldspar, in the biotite-rich samples, is interpreted to be the result of retrogression. As such, HO27BC and HO51 should record the highest equilibration temperatures, which were estimated at 800–900 °C at 5.5–7 kbar (Cesare et al. 1997; Álvarez-Valero and Kriegsman 2007).

The enclave from Mazarrón (AVMa8.9) contains the assemblage sillimanite–cordierite–garnet–K-feldspar–hercynite–biotite–plagioclase–graphite–ilmenite–glass. Hercynite occurs with cordierite and feldspars in coronae that have replaced garnet (Fig. 1c). These microstructures formed during decompression at ~820 ± 50 °C and 4.0 ± 0.4 kbar (Álvarez-Valero et al. 2007). Furthermore, a slight cooling event can be proposed, as suggested by the presence of symplectic biotite and plagioclase, probably formed by a melt-consuming reaction. Fresh glass in the rocks, with little or no evidence of crystallization during quenching, suggests that the microstructures are related to cooling phenomena predating eruption, e.g., residence in a relatively shallow magma chamber (Álvarez-Valero et al. 2007). A fast cooling rate

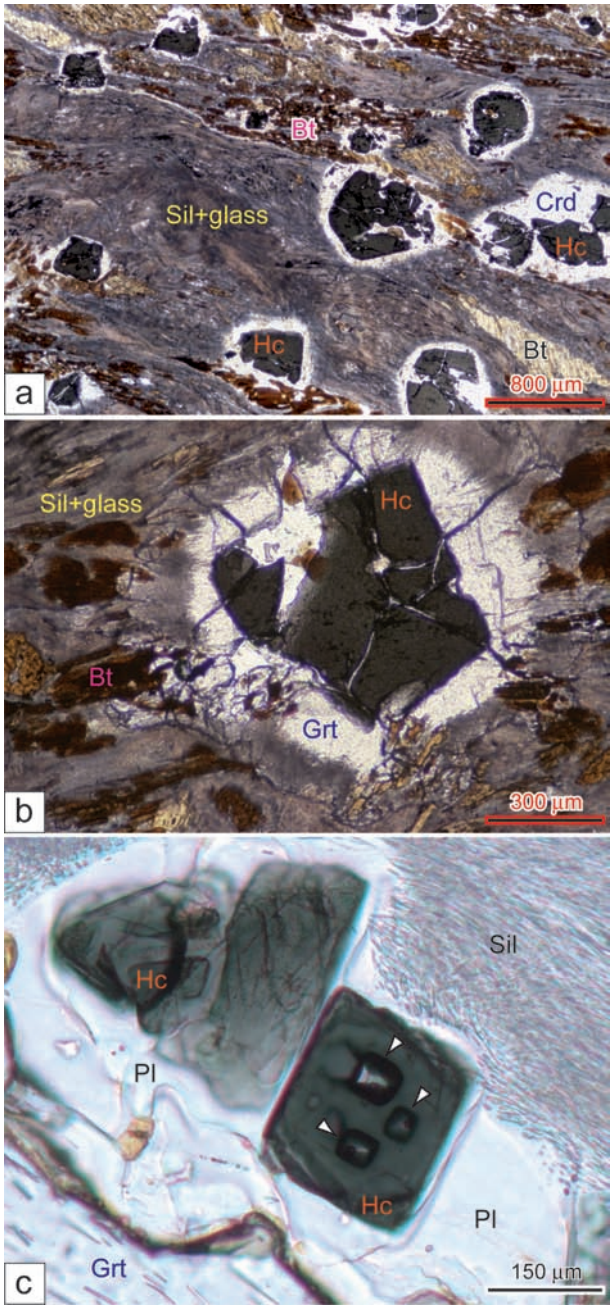

FIGURE 1. Plane-polarized light photomicrographs of spinel-cordierite enclaves from the Neogene Volcanic Province of SE Spain. (**a**) Typical appearance of spinel-cordierite enclaves from El Hoyazo: hercynite porphyroblasts with coronae of cordierite or K-feldspar statically overgrow a well-developed foliation marked by layers of biotite and acicular sillimanite intergrown with glass. (**b**) A porphyroblast of hercynitic spinel similar to those selected for this study. Here, the hercynite displays a corona of garnet. (**c**) Hercynite crystals forming coronae around garnet in an enclave from Mazarrón. The corona also contains plagioclase. Hercynite commonly contains inclusions of fresh glass (arrows) where one can recognize a small shrinkage bubble formed during cooling. Mineral abbreviations are after Kretz (1983).

of anatectic enclaves is suggested by the widespread presence of glass in these samples, as well as by melt inclusions within the spinel crystals (Fig. 1c).

Samples from the metamorphic complex, Lake Baikal, are laterites of Precambrian age, metamorphosed to amphibolite facies conditions. They are fine-grained rocks comprised mainly of almandine, sillimanite, corundum, hercynite, and ilmenite in varying proportions. Some thin (2–5 mm) layers contain abundant hercynite and ilmenite; other layers are rich with almandine-sillimanite/corundum-ilmenite. The chemical composition of these rocks is very well defined: high contents of Al_2O_3 (25–28%), TiO_2 (7–9%), and FeO (20%) with low contents of CaO and MgO (on average 1 and 2%, respectively) (Koneva 1988). This composition is comparable to modern lateritic material produced by the weathering of mafic rocks. The hercynite from Lake Baikal, occurring in hercynite-ilmenite layers with some admixture of feldspars, was separated by gravimetric technique using Clerici solution.

The samples studied here offer the opportunity to compare the cation distribution in hercynite from geological extremes of fast and slow cooling rates.

ANALYTICAL METHODS

Single-crystal diffraction data were collected using two four-circle diffractometers: a STOE AEDII diffractometer equipped with a point detector and a Stadi4-CCD diffractometer equipped with an area detector; both instruments, installed at the Department of Geosciences, University of Padova, work with Mo$K\alpha$ (0.71073 Å) radiation and a graphite monochromator. The unit-cell parameters of all crystals were determined with the point detector diffractometer by measuring the positions of the equivalents of the (4 0 0) and the (4 4 0) reflections on both sides of the incident beam. Diffraction intensities of the BK crystals were measured with the point detector diffractometer. Absorption corrections were calculated from Ψ-scans (North et al. 1968). Diffraction intensities of H&M crystals were collected with the area detector diffractometer. Numerical absorption corrections were applied (X-SHAPE software, Stoe and Cie 1998). Diffraction intensities were collected with the same coverage of the reciprocal space ($2\theta \leq 105°$).

The structure refinements were performed against F^2 using SHELXL-97 (Sheldrick 1997) with neutral O, Al, and Fe vs. Mg in the O, M, and T sites, respectively; refined parameters (Table 1) include the scale factor, secondary extinction coefficient (Ext), oxygen coordinate, tetrahedral and octahedral site occupancies, and displacement parameters.

Following X-ray data collection, the crystals were mounted on glass slides and polished for electron microprobe analysis. Grains were analyzed with a Cameca Camebax electron microprobe of the National Research Council-Institute of Geoscience and Georesources (C.N.R.-I.G.G.), Padova, using an accelerating potential voltage of 15 kV, a beam current of 20 nA, a beam diameter of 1 µm, and 20 s counting times. Synthetic oxides were used as standards. The data were corrected using the PAP correction method (Pouchou and Pichoir 1984). Ten to 14 analyses were performed for each sample; averages with standard deviations are reported in Table 2. Ferric iron content was calculated by charge balance and constraining the oxides wt% to 100.

Structural and chemical data were used to estimate cation distributions using the SIDR optimization algorithm described by Lavina et al. (2002). The procedure is essentially based on two assumptions: (1) the bond lengths are calculated as a linear combination of site atomic fractions (x_i) multiplied by their characteristic bond distances in spinel (except for Fe^{3+} and Ni^{2+}, which require additional considerations; see Lavina et al. 2002), and (2) the mean atomic number is a linear function of site atomic fractions multiplied by the atomic numbers. In the SIDR procedure, crystal-chemical parameters are calculated as a function of variable site atomic fractions and are forced to match observed parameters through minimization of the sum of squared differences between observed (O_j) and calculated (C_j) parameters divided by standard deviations (σ_j):

$$F(x_i) = 1/n \sum_{1}^{n} \left[\left(O_j - C_j(x_i) \right) / \sigma_j \right]^2 .$$

TABLE 1. Structural data

	H&M					BK	
	HO19	AVMa8.9	AVHz20	HO51	HO27BC	441A	441B
a (Å)	8.1584(5)	8.1511(4)	8.1517(6)	8.1504(5)	8.1474(6)	8.1460(6)	8.1451(5)
R_{eq} (%)	2.82	2.31	1.77	3.25	1.77	3.54	4.91
N_{meas}	2233	2228	2203	2242	2218	1686	1686
R_o (%)	3.63	2.01	1.18	3.88	1.26	3.81	3.06
$R_{4\sigma}$ (%)	2.22	1.88	1.66	1.97	1.56	2.2	1.42
$N_{4\sigma}$	142	152	169	140	160	152	144
R_{all} (%)	3.16	2.19	1.85	3.41	1.7	3.51	2.56
N_{all}	182	175	184	185	173	182	182
$wR2$ (%)	2.54	3.74	4.05	2.51	3.62	5.63	1.92
Goof	0.83	1.15	1.22	0.715	1.19	1.09	0.77
Ext	0.0126(4)	0.0132(7)	0.023(1)	0.0281(7)	0.0161(9)	0.013(2)	0.0129(3)
u	0.26371(8)	0.26393(7)	0.26405(6)	0.26352(7)	0.26385(6)	0.26471(7)	0.26464(6)
T-O (Å)	1.9580(11)	1.9614(10)	1.9632(9)	1.9554(1)	1.9594(9)	1.9712(10)	1.9703(8)
M-O (Å)	1.9322(6)	1.9309(5)	1.9302(5)	1.9337(5)	1.9306(5)	1.9242(5)	1.9243(4)
sof_M (Al)	0.0844(3)	0.0845(2)	0.0849(3)	0.0853(3)	0.0850(3)	0.0811(4)	0.08147(3)
sof_T (Fe)	0.02999(12)	0.03057(12)	0.03028(15)	0.02904(11)	0.02949(13)	0.0304(3)	0.02956(10)
UO (Å²)	0.0119(2)	0.01082(2)	0.0105(2)	0.0123(2)	0.0106(2)	0.0071(2)	0.00724(15)
UM (Å²)	0.00627(14)	0.00549(13)	0.00506(11)	0.00584(13)	0.00504(1)	0.0044(2)	0.00411(10)
$U_{12}M$ (Å²)					−0.00029(7)	−0.00034(9)	−0.00045(8)
UT (Å²)	0.00781(11)	0.00734(11)	0.00732(9)	0.00771(11)	0.00723(9)	0.00633(12)	0.00582(8)

Notes: The number of refined parameters is 8 or 9 with isotropic or anisotropic displacement parameters for M, respectively. *R* factors in %.

TABLE 2. Composition and optimized site atomic fractions, in atoms per formula units, of the single crystals

	H&M					BK	
	HO19	AVMa8.9	AVHz20	HO51	HO27BC	441A	441B
Al	1.963(10)	1.947(4)	1.906(4)	1.93(1)	1.922(7)	1.965(7)	1.944(7)
Fe^{2+}	0.842(4)	0.871(2)	0.857(4)	0.847(4)	0.832(4)	0.807(7)	0.785(4)
Mg	0.137(5)	0.116(3)	0.144(3)	0.149(3)	0.164(4)	0.189(4)	0.206(3)
Fe^{3+}	0.036(11)	0.051(5)	0.075(5)	0.05(1)	0.059(8)	0.031(6)	0.051(6)
Ti	n.d.	n.d.	0.006(1)	0.006(1)	0.005(1)	n.d.	0.001(1)
Zn	0.021(3)	0.013(2)	0.002(2)	0.004(2)	0.004(1)	0.004(2)	0.008(2)
Si	n.d.	n.d.	0.002(1)	0.001(1)	0.001(1)	n.d.	n.d.
Cr	0.001(1)	0.002(1)	0.001(1)	0.002(1)	0.002(2)	n.d.	n.d.
Mn	n.d.	n.d.	0.005(2)	0.007(1)	0.007(1)	n.d.	0.001(1)
V	n.d.	n.d.	0.002(1)	0.004(2)	0.004(1)	0.004(1)	0.003(1)
Fe^{3+}/Fe_{tot}	0.041	0.055	0.08	0.055	0.066	0.037	0.061
Tetrahedral cations optimized assuming random Fe^{3+} distribution							
$F(x_i)$*	1.9	0.8	0.1	0.4	0.2	0.4	0.6
Al	0.17	0.16	0.14	0.18	0.16	0.11	0.11
Fe^{2+}	0.75	0.77	0.77	0.73	0.74	0.77	0.76
Mg	0.05	0.04	0.06	0.06	0.07	0.10	0.11
Fe^{3+}	[0.01]	[0.01]	[0.02]	[0.02]	[0.02]	[0.01]	[0.02]
i†	0.19	0.17	0.16	0.20	0.18	0.12	0.13

Notes: n.d. = not detected.
* Sum of squared differences between observed and calculated parameters(see text).
† Inversion parameter defined as sum of trivalent cations in the tetrahedral site.

The small amounts of Ti, Cr, and V were constrained to the M site, whereas Si, Zn, and Mn were constrained to the T site.

The small value of the minimization function obtained for all samples implies that experimental parameters were successfully recalculated which, in turn, implies that the adopted model is good enough to reproduce experimental values. Moreover the small value of the minimization function indicates that the chemical data matches the structural data; non-representative chemical data due to crystal inhomogeneity or an error in the estimation of the Fe^{2+}/Fe^{3+} ratio would result in incorrect lattice parameters. However, a small value of the minimization function does not necessarily imply that the site atomic fractions are estimated with great accuracy. To test how the four exchanging cations are actually constrained in the optimization, the value of the minimization function was scanned at fixed $^{IV}Fe^{3+}$ values, with the other atomic fractions set as variable. Results are summarized in Figure 2a. $F(x_i)$ is almost flat over the entire range of $^{IV}Fe^{3+}$. Only a complete tetrahedral ordering in one of the BK crystals led to a significant worsening of the fit, showing that the distribution of $^{IV}Fe^{3+}$ is very poorly constrained. Therefore Fe^{3+} was set to a random distribution and the site fractions of Mg, Al, and Fe^{2+} were optimized. The distribution of these three cations is affected by the Fe^{3+} distribution (Fig. 2b) but, as discussed in Uchida et al. (2005), the inversion parameter shows limited variation, around 0.02. In fact, the total Fe content in each site, and the amount of the smaller (Fe^{3+} + Al) vs. larger cations (Mg + Fe^{2+}), are well constrained by the site scattering power and bond lengths, respectively. A reasonable error for the estimation of site atomic fraction is ~0.01 apfu (Lavina et al. 2002).

RESULTS

The crystals can be ascribed to the hercynite-spinel join with a minor spinel ferrite component. The generalized chemical formula is $(Fe^{2+}, Mg)(Al, Fe^{3+})_2O_4$, with $1.91 < Al < 1.96$, $0.78 < Fe^{2+} < 0.87$, $0.12 < Mg < 0.21$, $0.03 < Fe^{3+} < 0.07$. The substitutions Fe^{2+}-Mg and Al-Fe^{3+} are common in hercynite. Crystals are chemically homogeneous, as evidenced by the low standard deviations on element concentrations (Table 2). BK crystals are slightly richer in Mg (spinel component) than H&M crystals and consequently exhibit smaller cell volumes. Cell parameters of the hercynite and spinel end-members are given as 8.1458(6) Å (Harrison et al. 1998) and 8.0832(5) Å (Fischer 1967), respectively. The cell edge is correlative to the total Fe content (Fig. 3), representing the two largest isomorphic substitutions, Mg-Fe^{2+} and Al-Fe^{3+}; both involve the substitution of smaller for larger

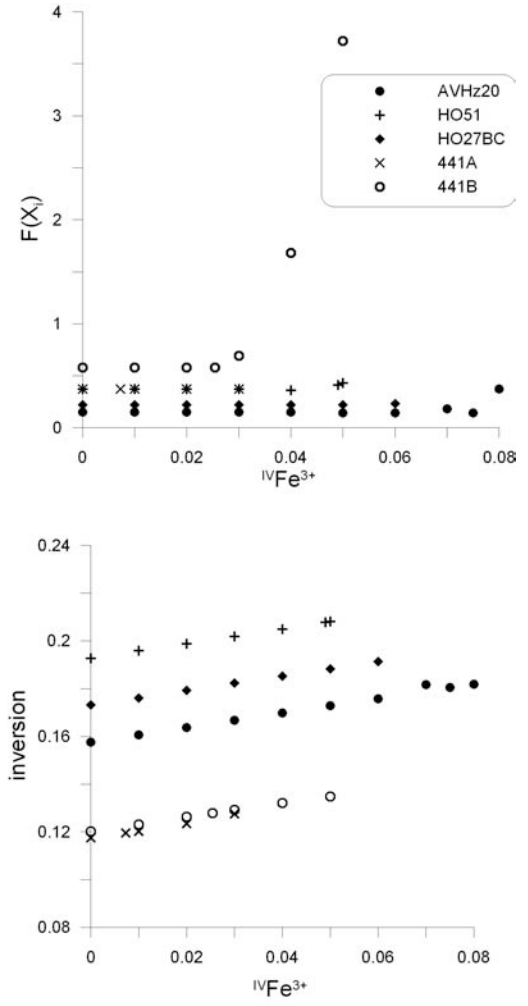

Figure 2. Plot of the minimization function (**a**) and of the inversion parameter (**b**) obtained by optimizing the distribution of Mg, Al, and Fe^{2+} with $^{IV}Fe^{3+}$ fixed at the values in abscissa. The minimization function does not change significantly over a wide range of $^{IV}Fe^{3+}$, the only exception is 441B hercynite, which seems to preclude complete tetrahedral Fe^{3+} ordering.

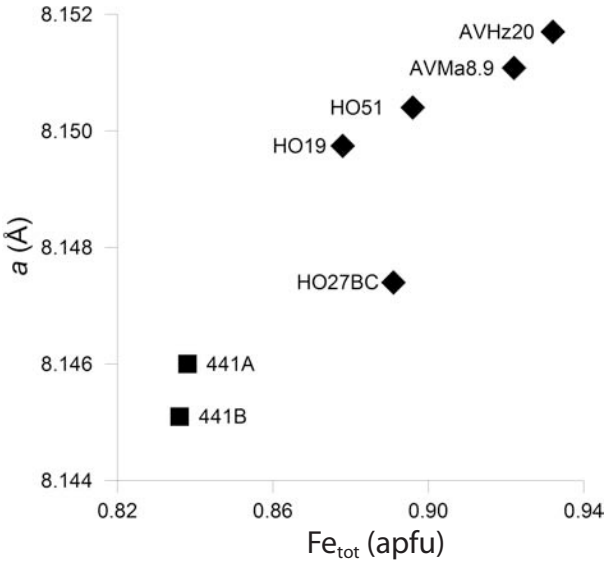

Figure 3. Variation of the lattice parameter as a function of the total iron content.

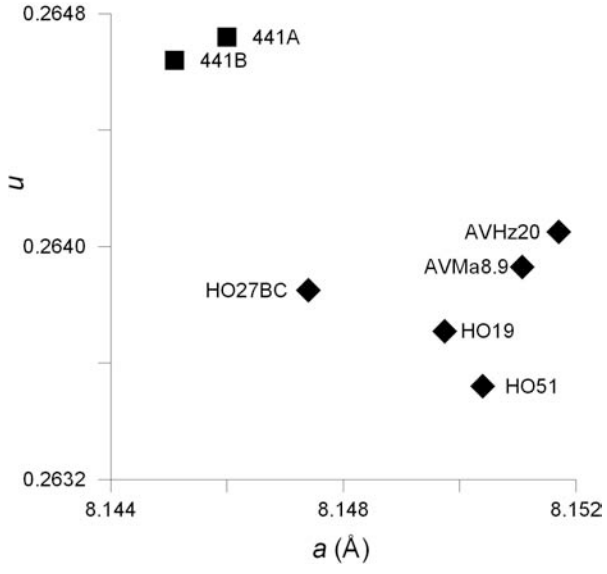

Figure 4. Oxygen fractional coordinate vs. lattice parameter.

cations. BK crystals exhibit larger oxygen fractional coordinates than H&M crystals, which is shown later to be related to the larger intracrystalline ordering (Larsson et al. 1994; Harrison et al. 1998). Crystals from anatectic rocks show a range in lattice parameter (*a*) and fractional coordinate (*u*) (Fig. 4) due to both compositional differences and different cooling rates.

Comparative crystal chemistry and closure temperature

The ordering on cooling of the natural samples likely occurred in different stages according to the different kinetics of the short-range diffusion of the exchanging cations. Concerning the four major cations, a tentative sequence of the kinetics of intracrystalline exchanges could be Fe^{2+}-Al ≈ Mg-Al < Mg-Fe^{3+} < Fe^{2+}-Fe^{3+}; each reaction potentially bearing information about different stages along the cooling history. Unfortunately the distribution of the four major cations has not been determined with sufficient accuracy to model the distribution of each of them. However the modeling includes, together with the end-members, the Fe^{3+}-bearing Hc-Spl solid solution by Andreozzi and Lucchesi (2002), so that the effect of Fe^{3+} is to some extent empirically accounted for.

Although the Fe^{3+} effect is not modeled in this study, it is worth discussing its possible behavior in the ordering process. Ferric iron might play a unique role in the intracrystalline ordering and inversion parameter interpretation considering that: (1) the Fe^{2+}-Fe^{3+} exchange is not quenchable (Harrison and Putnis 1999); (2) the ordering stages are not necessarily independent (i.e., on cooling, the ordering of diffusing cations

can be affected by the intracrystalline distribution of other ions, the ordering of which is kinetically hindered); and (3) it is not obvious from the literature whether Fe^{3+} has a preference for T or M sites for low amounts of Fe^{3+} in Mg-Al-Fe^{2+} spinel. Ferric iron shows tetrahedral site preference in magnetite and magnesioferrite end-members and in Fe^{3+}-rich spinels along the spinel-magnesioferrite join (Nakatsuka et al. 2004), where *i* decreases with increasing *T*. If Fe^{3+} also has a preference for tetrahedral coordination in the studied system, i.e., if there is a mixing between two normal spinels (hercynite and magnesite) and an inverse one (magnetite), the inversion parameter would be increased with respect to the spinel-hercynite solid solution at any temperature, and therefore would give an overestimation of T_C interpreted neglecting the Fe^{3+} component. In contrast, if Fe^{3+} has a preference for octahedral coordination, as suggested by Della Giusta et al. (1996) and Andreozzi and Lucchesi (2002), the inversion parameter could be properly interpreted as in a solid solution between normal end-member spinels. Recalling that in the four cation system, $i = {}^{IV}Al + {}^{IV}Fe^{3+} = {}^{VI}Mg + {}^{VI}Fe^{2+}$, and considering that the $^{IV}Fe^{3+}$ in the studied spinels is unknown but potentially contributes up to 30% of the inversion parameter (see Table 2), it is clear that even small Fe^{3+} substitution can play a major role in the interpretation of *i* values.

Modeling

In our modeling, the system is simplified to the hercynite-spinel join where Al should be the slowest diffusing cation because it is the most strongly bonded and because of the kinetics of the ordering processes (the Fe^{2+}-Al and the Mg-Al exchanges) should be mainly controlled by Al. Structural (the oxygen fractional coordinate, *u*), chemical [the hercynite component, $Hc = Fe^{2+}/(Mg + Fe^{2+})$] and ordering (the inversion degree, *i*) parameters are compared with those from the literature in order to estimate the closure temperature, T_C, of the samples. The interpretation of the solid solution in terms of end-member behavior is supported by the following: (1) in spinel (Andreozzi et al. 2000) and in hercynite (Harrison et al. 1998), *u* shows a quasi-linear negative trend with the equilibration temperature; (2) *i* shows a quasi-linear positive trend with the equilibration temperature in both end-members; and (3) the inversion parameters of the end-members of the spinel-hercynite samples by Andreozzi and Lucchesi (2002), interpreted by the authors as having a homogeneous equilibration temperature of ~800 °C, show a linear variation along the join of *u* and a slight deviation from the linearity of *i*.

The oxygen fractional coordinates, *u*, of BK samples are significantly larger than those of the H&M samples. Since *u* has a negative correlation with *T* in spinel and hercynite, it can be inferred that BK crystals record a much lower T_C, in agreement with the geological settings of the samples. Structural and chemical data of sample HO27BC are close to the data of sample He9a/h from Andreozzi and Lucchesi (2002), so its T_C should be close to 800 °C, the equilibration temperature given by Andreozzi and Lucchesi (2002) for their samples.

To perform a quantitative estimate of T_C, *u*-Hc-*T* (equilibration temperature) data by Andreozzi et al. (2000) (spinel), Harrison et al. (1998) (hercynite), and Andreozzi and Lucchesi (2002) (spinel-hercynite s.s.) have been fitted to a plane equation:

$$T\,(°C) = T_0 + k_1\,Hc + k_2\,u, \quad (1)$$

with T_0, k_1, and k_2 fitted parameters (Table 3, Fig. 5). The values of *u* from the high-temperature in situ data of Harrison et al. (1998) were recalculated to ambient *T* by applying thermal expansion effects (Hazen and Prewitt 1977). The fitted equation was then applied to the data from the natural samples in this study, and the results are given in Table 3. Calculated T_C for BK samples are around 400 °C. A minimum error in calculated T_C has been estimated at about 30 °C, assuming that the only sources of

TABLE 3. Closure temperatures and fitting coefficients calculated from structural and chemical parameters (equations in the text)

	Calculated closure temperatures (°C)		
	Equation 1	Equation 2	Equation 3
		H&M samples	
HO19	860	900	880
AVMa8.9	780	810	800
AVHz20	710	760	730
HO51	930	940	920
HO27BC	780	840	820
		BK samples	
441A	400	550	510
441B	410	590	550
		Fitting parameters	
R^2 (%)*	91	91	96
T_0†	1.12×10^5	−315	−310
k_1†	807	380	6
k_2†	-4.242×10^5	4.75×10^3	4.8×10^3
k_3†			370

* Coefficient of determination.
† Fitted coefficients of functions given in the text; 30 data points from the literature (see text) were used for the fittings.

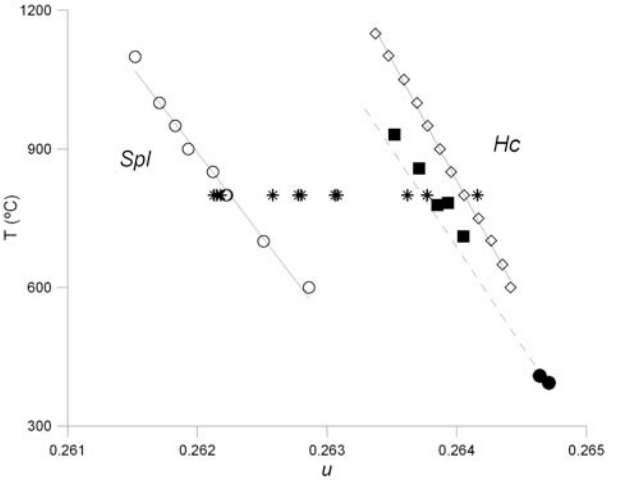

FIGURE 5. Temperature (experimental-equilibration temperatures and calculated-closure temperatures) vs. oxygen fractional coordinate. Solid squares and solid circles = T_C of H&M and BK calculated from *u* and Hc values; open circles, asterisks, diamonds = equilibration temperature data for spinel (Andreozzi et al. 2000), Spl-Hc solid solution (Andreozzi and Lucchesi 2002), and hercynite (Harrison et al. 1998), respectively, the latter recalculated to room temperature. The dashed lines show the calculated behavior of the solid solution $Hc_{80}Spl_{20}$.

uncertainty are the experimental errors on u and Hc.

If Al is the limiting factor in intracrystalline ordering, hercynite that equilibrated in slow cooled metamorphic environments should show a value of T_C close to that of Mg-Al spinels equilibrated under similar conditions. T_C has been estimated to be ~450 °C for metamorphic spinels from Lake Baikal (Lavina et al. 2003). Therefore, estimated values of T_C obtained for BK are plausible. The T_C for H&M samples ranges from ~700 to ~950 °C. The estimated temperatures are consistent with the anatectic nature of the samples, where non-homogeneous cooling rates are expected. The T_C calculated for H&M crystals are comparable with fast cooling rates of the host lavas during submarine extrusion.

An approach similar to that described for the T-Hc-u data has been conducted for the modeling of the T-Hc-i data. The fitting was performed with either an equation of a plane (Eq. 2) or the introduction of a quadratic term for Hc (Eq. 3) to take into account the non-linear trend of i vs. Hc at 800 °C observed by Andreozzi and Lucchesi (2002):

$$T_C\,(°C) = T_0 + k_1\,Hc + k_2\,i \quad (2)$$

$$T_C\,(°C) = T_0 + k_1\,Hc + k_2\,i + k_3\,Hc^2 \quad (3)$$

A graphical representation of the fitting results is provided in Figure 6 and values are reported in Table 3. Adopting Equation 3 implies that the "i excess" of the solid solution at 800 °C extends throughout the investigated T range. The fitting of four parameters for this model is not constrained by the data, but it is still interesting to examine the results. The two models produce similar T_C values, except that T_C is 20 to 40 °C lower when using Equation 3. An estimation of the minimum uncertainty, propagating errors on Hc and i, and considering $\sigma(i) = 0.01$ (see analytical section), gives $\sigma(T_C) = 70$ °C, more than twice as large as with Equation 1.

The values of T_C calculated for H&M are comparable to those obtained from the u modeling. The calculated temperatures for BK samples, ~550 °C, seem too high with respect to the geological setting. Besides experimental errors such as an overestimation of i in BK samples, possible explanations for the overestimation of T_C could be a large deviation from linearity of i vs. Hc of the solid solution at low temperature or the Fe^{3+} effect discussed above and not properly accounted for due to experimental limitations. Notably, assuming a tetrahedral site preference for Fe^{3+}, would have remarkably lowered the calculated T_C.

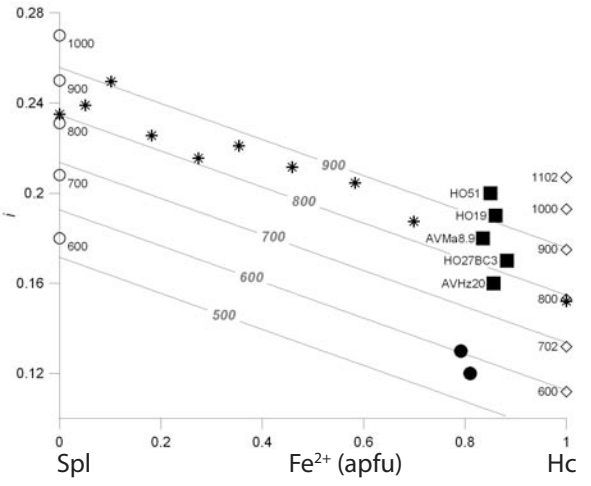

FIGURE 6. Two-dimensional projection of the i-Hc-T plane (fit b in Table 3) with plotted isotherms for 500, 600, 700, 800, and 900 °C. Full circles = BK samples, full squares = H&M samples. Open circles = Andreozzi et al. (2000); open diamonds = Harrison et al. (1998); asterisks = Andreozzi and Lucchesi (2002).

Discussion

In light of calculated T_C values having an uncertainty of ~50 °C, it is worthy to discuss their geologic relevance, with reference to the anatectic H&M crustal enclave samples. It is important to take into account that T_C (the temperature at which intracrystalline cation ordering ceases) is lower than the temperature of growth or equilibration of hercynite in the enclaves (as calculated by petrologic thermometry; see Cesare et al. 1997; Álvarez-Valero et al. 2005, 2007; Álvarez-Valero and Kriegsman 2007), and may equal this value only in the case of infinite cooling rates. With this perspective, T_C represents an independent, useful tool for thermometric studies in very rapidly cooled samples, such as xenoliths and enclaves in lavas. In such samples, T_C provides a minimum equilibration temperature, in a manner similar to the ternary feldspar thermometer. In the studied H&M enclaves, the highest T_C of ~900 °C calculated for sample HO51 overlaps (within error) the maximum temperatures inferred for the hercynite-bearing enclaves (Cesare et al. 1997; Cesare 2000; Ferri et al. 2007), and suggests that (some) enclaves reached temperatures approaching 900 °C. This also indicates that HO51 had an extremely fast cooling rate.

Variations in T_C indicate differences in cooling rate and/or in initial temperature of the sample. If the highest values of T_C indicate the temperatures at which the enclaves were residing deep in the crust just before lava extrusion, then the overall large range, reaching values as low as 670 °C, suggests that the five H&M samples did not share a common history, at least in the final cooling stage (see different P-T histories in Álvarez-Valero and Kriegsman 2007). Given their small size and the absence of reaction rims at the contact with the host lava, enclaves must have been thermally equilibrated with the lava during extrusion. Therefore, the most plausible explanation for the range in T_C is differences in cooling rate among the various portions of the volcanic edifices. Even if El Hoyazo was a relatively small lava dome (~1 km in diameter and few hundred meters in height), we can expect notable variations in cooling times (minutes to hours, probably days) among its most external (higher T_C) and deepest parts (lower T_C). At Mazarrón, where volcanic rocks extend over ~100 km^2, the possibility that the cooling of lavas was slower is even greater, and is consistent with the lower T_C of sample AVMa8.9. The role of differences in the temperature of lava extrusion cannot be excluded, but is very difficult to constrain. In any case, given the rather constant chemical and petrographic composition of lavas at El Hoyazo, differences in lava temperature might account for a few tens of degrees, and not for the measured range of T_C, exceeding 250 °C.

CONCLUDING REMARKS

Comparing data of natural and synthetic samples for the estimation of the closure temperature necessarily requires some assumptions and approximations. In this study, minor substitutional elements are neglected and experimental trends of synthetic samples from the literature are extrapolated to conditions that are not reproducible in the laboratory, such as the degree of ordering of the slowly cooled natural samples. Moreover, the cation distribution of a solid solution results from different ordering processes with different kinetics that are not necessarily independent. These simplifications must be considered when critically evaluating the results. On the other hand, if the complexity of the natural system were fully unraveled, a more complete set of information on the cooling history could be extracted rather than a closure temperature alone.

The samples investigated here show close to the largest order and disorder observable in natural hercynite. Accordingly, their oxygen fractional coordinate and degree of ordering show important differences. The quantitative estimation of T_C based on the u values seems to be more reliable than the one based on the i values, at least for the slow-cooled samples. This is likely due to the inherent experimental uncertainty in the cation distribution determination in the solid solution, while the oxygen fractional coordinate is a sensitive and robust parameter from the structural refinement.

ACKNOWLEDGMENTS

We thank Henrik Skogby and an anonymous reviewer for their constructive comments. Support from NSF-EAR-0622171, NSF-DMR-0521179, and DE-FG02-94ER14466 to B.L., and from Italian MIUR (grant PRIN 2007278A22) and C.N.R. (Euromargins ESF Eurocore) to B.C., is gratefully acknowledged. Fieldwork was supported by the Russian Foundation for Basic Research (grant RFBR 06-05-64300). A.V. thanks JAE-Doc program (CSIC-2007).

REFERENCES CITED

Acosta-Vigil, A., Cesare, B., London, D., and Morgan, G.B. (2007) Microstructures and composition of melt inclusions in a crustal anatectic environment, represented by metapelitic enclaves within El Hoyazo dacites, SE Spain. Chemical Geology, 237, 450–465.

Álvarez-Valero, A.M. and Kriegsman, L.M. (2007) Crustal thinning and mafic underplating beneath the Neogene Volcanic Province (Betic Cordillera, SE Spain): evidence from crustal xenoliths. Terra Nova, 19, 266–271.

Álvarez-Valero, A.M., Cesare, B., and Kriegsman, L.M. (2005) Formation of elliptical garnet in a metapelitic enclave by melt-assisted dissolution and reprecipitation. Journal of Metamorphic Geology, 23, 65–74.

——— (2007) Formation of spinel-cordierite-feldspar-glass coronas after garnet in metapelitic xenoliths: Reaction modeling and geodynamic implications. Journal of Metamorphic Geology, 25, 305–320.

Andreozzi, G.B. and Lucchesi, S. (2002) Intersite distribution of Fe^{2+} and Mg in the spinel (sensu stricto)-hercynite series by single-crystal X-ray diffraction. American Mineralogist, 87, 1113–1120.

Andreozzi, G.B. and Princivalle, F. (2002) Kinetics of cation ordering in synthetic $MgAl_2O_4$ spinel. American Mineralogist, 87, 838–844.

Andreozzi, G.B., Princivalle, F., Skogby, H., and Della Giusta, A. (2000) Cation ordering and structural variations with temperature in $MgAl_2O_4$ spinel: An X-ray single-crystal study. American Mineralogist, 85, 1164–1171.

Bohlen, S.R., Dollase, W.A., and Wall, V.J. (1986) Calibration and applications of spinel equilibria in the system FeO-Al_2O_3-SiO_2. Journal of Petrology, 27, 1143–1156.

Carbonin, S., Russo, U., and DellaGiusta, A. (1996) Cation distribution in some natural spinels from X-ray diffraction and Mössbauer spectroscopy. Mineralogical Magazine, 60, 355–368.

Cesare, B. (2000) Incongruent melting of biotite to spinel in a quartz-free restite at El Joyazo (SE Spain): Textures and reaction characterization. Contributions to Mineralogy and Petrology, 139, 273–284.

Cesare, B., Mariani, E.S., and Venturelli, G. (1997) Crustal anatexis and melt extraction during deformation in the restitic xenoliths at El Joyazo (SE Spain). Mineralogical Magazine, 61, 15–27.

Cesare, B., Marchesi, C., Hermann, J., and Gomez-Pugnaire, M.T. (2003) Primary melt inclusions in andalusite from anatectic graphitic metapelites: Implications for the position of the Al_2SiO_5 triple point. Geology, 31, 573–576.

Da Rocha, S. and Thibaudeau, P. (2003) Ab initio high-pressure thermodynamics of cationic disordered $MgAl_2O_4$ spinel. Journal of Physics: Condensed Matter, 15, 7103–7115.

Della Giusta, A., Princivalle, F., and Carbonin, S. (1986) Crystal chemistry of a suite of natural Cr-bearing spinels with $0.15 \le Cr \le 1.07$. Neues Jahrbuch für Mineralogie, Abhandlungen, 155, 319–330.

Della Giusta, A., Carbonin, S., and Ottonello, G. (1996) Temperature-dependent disorder in a natural Mg-Al-Fe^{2+}-Fe^{3+}-spinel. Mineralogical Magazine, 60, 603–616.

Ferri, F., Burlini, L., Cesare, B., and Sassi, R. (2007) Seismic properties of lower crustal xenoliths from El Hoyazo (SE Spain): Experimental evidence up to partial melting. Earth and Planetary Science Letters, 253, 239–253.

Fischer, P. (1967) Neutronenbeugungsuntersuchung der Strukturen von $MgAl_2O_4$- und $ZnAl_2O_4$-spinellen, in Abhangigkeit von der Vorgeschichte. Zeitschrift für Kristallographie, 115, 275–302.

Ganguly, J. (1982) Mg-Fe order-disorder of ferromagnesian silicates. II. Thermodynamics, kinetics, and geological applications. In S.K. Saxena, Ed., Advances in Physical Geochemistry, 2, p. 58–99. Springer, Berlin.

Hålenius, U., Skogby, H., and Andreozzi, G.B. (2002) Influence of cation distribution on the optical absorption spectra of Fe^{3+}-bearing spinel s.s.-hercynite crystals: evidence for electron transitions in $^{VI}Fe^{2+}$-$^{VI}Fe^{3+}$ clusters. Physics and Chemistry of Minerals, 29, 319–330.

Harrison, R.J. and Putnis, A. (1997) Interaction between exsolution microstructures and magnetic properties of the magnetite-spinel solid solution. American Mineralogist, 82, 131–142.

——— (1999) The magnetic properties and crystal chemistry of oxide spinel solid solutions. Surveys in Geophysics, 19, 461–520.

Harrison, R.J., Redfern, S.A.T., and O'Neill, H.St.C. (1998) The temperature dependence of the cation distribution in synthetic hercynite ($FeAl_2O_4$) from in situ neutron structure refinements. American Mineralogist, 83, 1092–1099.

Harrison, R.J., Dove, M.T., Knight, K.S., and Putnis, A. (1999) In situ neutron diffraction study of non-convergent cation ordering in the $(Fe_3O_4)_{1-x}(MgAl_2O_4)_x$ spinel solid solution. American Mineralogist, 84, 555–563.

Hazen, R.M. and Prewitt, C.T. (1977) Effects of temperature and pressure on interatomic distances in oxygen-based minerals. American Mineralogist, 62, 309–315.

Hill, R.J. (1984) X-ray powder diffraction profile refinement of synthetic hercynite. American Mineralogist, 69, 937–942.

Koneva, A.A. (1988) About Precambrian crust of weathering in Priolkhonje (West Baikal Region). Doklady Akademii Nauk, 302(5), 1217–1220 (in Russian).

Kretz, R. (1983) Symbols for rock-forming minerals. American Mineralogist, 68, 277–279.

Larsson, L., O'Neill, H.St.C., and Annersten, H. (1994) Crystal chemistry of synthetic hercynite ($FeAl_2O_4$) from XRD structural refinements and Mössbauer spectroscopy. European Journal of Mineralogy, 6, 39–51.

Lavina, B., Salviulo, G., and Della Giusta, A. (2002) Cation distribution and structure modeling of spinel solid solutions. Physics and Chemistry of Minerals, 29, 10–18.

Lavina, B., Koneva, A., and Della Giusta, A. (2003) Cation distribution and cooling rates of Cr-substituted Mg-Al spinel from the Olkhon metamorphic complex, Russia. European Journal of Mineralogy, 15, 435–441.

Makrygina, V.A., Petrova, Z.I., Koneva, A.A., and Suvorova, L.F. (2008), Composition, *P-T* parameters, and metasomatic transformations of mafic schists of the Svyatoi Nos Peninsula, Western Baikal Area. Geochemistry International, 46, 140–155.

Méducin, F., Redfern, S.A.T., Le Godec, Y., Stone, H.J., Tucker, M.G., Dove, M.T., and Marshall, W.G. (2004) Study of cation order-disorder in $MgAl_2O_4$ spinel by in situ neutron diffraction up 1600 K and 3.2 GPa. American Mineralogist, 89, 981–986.

Nakatsuka, A., Ueno, H., Nakayama, N., Mizota, T., and Maekawa, H. (2004) Single-crystal X-ray diffraction study of cation distribution in $MgAl_2O_4$-$MgFe_2O_4$ spinel solid solution. Physics and Chemistry of Minerals, 31, 278-287.

North, A.C.T., Phillips, D.C., and Scott-Mattews, F. (1968) A semiempirical method of absorption correction. Acta Crystallographica A, 24, 351–352.

O'Neill, H.St.C. (1994) Temperature dependence of the cation distribution in $CoAl_2O_4$ spinel. European Journal of Mineralogy, 6, 603–609.

O'Neill, H.St.C. and Dollase, W.A. (1994) Crystal structures and cation distributions in simple spinels from powder XRD structural refinements: $MgCr_2O_4$, $ZnCr_2O_4$, Fe_3O_4 and the temperature dependence of the cation distribution in $ZnAl_2O_4$. Physics and Chemistry of Minerals, 20, 541–555.

O'Neill, H.St.C. and Navrotsky, A. (1984) Cation distribution and thermodynamic properties of binary spinel solid solutions. American Mineralogist, 69, 733–753.

O'Neill, H.St.C., Annersten, H., and Virgo, D. (1992) The temperature dependence of the cation distribution in magnesioferrite ($MgFe_2O_4$) from powder XRD structural refinements and Mössbauer spectroscopy. American Mineralogist, 77, 725–740.

Peterson, R.C., Lager, G.A., and Hitterman, R.L. (1991) A time-of-flight neutron powder diffraction study of $MgAl_2O_4$ at temperatures up to 1273 K. American Mineralogist, 76, 1455–1458.

Pouchou, J.L. and Pichoir, F. (1984) A new model for quantitative X-ray-microanalysis. 1. Application to the Analysis of Homogeneous Samples. La Recherche Aérospatiale, 3, 167–192.

Princivalle, F., Della Giusta, A., and Carbonin, S. (1989) Comparative crystal chemistry of spinels from some suites of ultramafic rocks. Mineralogy and Petrology, 40, 117–126.

Redfern, S.A.T., Harrison, R.J., O'Neill, H.St.C., and Wood, D.R.R. (1999) Thermodynamics and kinetics of cation ordering in $MgAl_2O_4$ spinel up to 1600 °C from in situ neutron diffraction. American Mineralogist, 84, 299–310.

Sheldrick, G.M. (1997) SHELX97. University of Gottingen, Germany.

Stoe and Cie (1998) X-SHAPE. Stoe and Cie, Darmstadt, Germany.

Uchida, H., Lavina, B., Downs, R.T., and Chesley, J. (2005) Single-crystal X-ray diffraction of spinels from the San Carlos Volcanic Field, Arizona: Spinel as a geothermometer. American Mineralogist, 90, 1900–1908.

Waerenborgh, J.C., Figueiredo, M.O., Cabral, J.M.P., and Pereira, L.C.J. (1994a) Powder XRD structure refinements and ^{57}Fe Mössbauer effect study of synthetic $Zn_{1-X}Fe_xAl_2O_4$ ($0- < x \leq -1$) spinels annealed at different temperatures. Physics and Chemistry of Minerals, 21, 460–468.

——— (1994b) Temperature and composition dependence of the cation distribution in synthetic $ZnFe_yAl_{2-y}O_4$ ($0 \leq y \leq 1$) Spinels. Journal of Solid State Chemistry, 111, 300–309.

Zeck, H.P. (1970) An erupted migmatite from Cerro del Hoyazo, SE Spain. Contributions to Mineralogy and Petrology, 26, 225–246.

Manuscript received June 1, 2008
Manuscript accepted January 19, 2009
Manuscript handled by Laurence Galoisy